



# Process-dependent persistence in precipitation records

Lichao Yang, Zuntao Fu\*

Lab for Climate and Ocean-Atmosphere Studies, Department of Atmospheric and Oceanic Sciences, School of Physics, Peking University, Beijing, 100871, China



## HIGHLIGHTS

- Precipitation records of multiple temporal resolutions are analyzed.
- Precipitation takes two distinct scaling regimes over different scales.
- Precipitation persistence over different scales is process-dependent.

## ARTICLE INFO

### Article history:

Received 17 January 2019

Received in revised form 2 April 2019

Available online 10 May 2019

### Keywords:

Precipitation persistence

Process-dependent

Scaling regime

## ABSTRACT

Whether long-term persistence (LTP) exists in precipitation process has been studied for several decades and it is still an open question. In this study, the precipitation records of hourly and daily resolutions are applied to estimate the persistence of precipitation over a wider range of scales mainly by means of Detrended Fluctuation Analysis (DFA). The results show that precipitation persistence can be described as a varying rather than a universal scaling behavior. Two distinct scaling regimes are determined by their associated power law behavior ( $F(s) \propto s^\alpha$ ,  $F(s)$  is the fluctuation function,  $s$  is the time scale,  $\alpha$  is the scaling exponent) and they are process-dependent: a regime of frontal systems with stronger LTP ( $s$  is less than around 200 h,  $\alpha \approx 0.74$ ) and a regime of random nature of weather system and climate variability with weaker LTP ( $s$  is larger than around 200 h,  $\alpha \approx 0.54$ ). This result indicates that when we simulate the precipitation process, it is necessary to take the different persistent properties over the corresponding scale range into account to select the appropriate model.

© 2019 Elsevier B.V. All rights reserved.

## 1. Introduction

Long-term persistence (LTP), also called long-term correlation (LTC), long-term memory (LTM) means that the present states of a system may have a further influence on the states in the future. One can simply explain it by using autocorrelation function  $C(s)$ . If the autocorrelation function  $C(s)$  of a time series decays as a power law,  $C(s) \sim s^{-\gamma}$ , then the typical correlation time is not integrable and we can consider it long-term correlated [1]. Studies show that the LTP exists in the time series of several climatological and hydrological variables such as temperature and river runoff [2–8].

While the LTP in climatological and hydrological systems has been discussed for decades, the existence in long-term persistence of precipitation is still under debate. The difficulty arises from the complex structures and wide range of temporal and spatial scales of precipitation as precipitation involves various complex atmospheric processes, including storms, frontal systems and seasonal fluctuations [9–13].

\* Corresponding author.

E-mail address: [fuzt@pku.edu.cn](mailto:fuzt@pku.edu.cn) (Z. Fu).

The first study for long-term persistence of precipitation dates back to 1956, when Hurst found that Hurst exponent of precipitation records indicated long-term persistence [2]. Later, Potter applied autocorrelation function and found the annual precipitation is a short-memory process [3]. More recently, the growing number of precipitation datasets with long-term records and newly developed methods allow further investigation of the long-term statistical analysis on precipitation. However, the results are still controversial in the literature. Using the daily instrumental precipitation records, previous studies pointed out that the precipitation process presents a weakly correlated behavior by the method of Detrended Fluctuation Analysis (DFA), rescaled range analysis and periodogram [10,11,13–15]. However, on the basis of power spectra analysis, the ensemble averaged power spectra of precipitation exhibit distinct scaling regimes: white noise at intermediate scales (from one month to three years) and LTP on scales larger than three years [4]. Moreover, with the development of precipitation reconstructions, many studies found long-term persistence exists in the precipitation reconstructions and model simulations. Bunde compared proxy-based reconstructions with model simulations and instrumental records at the same geographic areas [12]. They found instrumental precipitation observations behave like white noise, while a long-term persistence behavior exists in the reconstruction datasets. It is in good agreement with the results found by Markonis and Koutsoyiannis, who insist that precipitation persistence in the reconstruction datasets is scale-dependent. Below decadal time scales, it presents as white noise or Markov-typed process. When it comes to multi-decadal timescales, the long-term persistence or Hurst–Kolmogorov (HK) behavior emerges [16].

So whether the precipitation process presents long-term persistence is still an open question. The conflicts result from the different sampled datasets, the limited observation records or inappropriate applied methods. First of all, different resolution precipitation records have been considered in the literature, such as 5-minute or 15-minute precipitation records [4] [9], daily or monthly precipitation records [10–13,15,17], and even annual precipitation records [3]. Finer resolution sampled precipitation can keep the detailed structures on the smaller time scales. Coarse resolution sampled precipitation will filter off these details. So different resolution sampled precipitation records with different data length will present different correlation structures of precipitation. Secondly, the sequences of high-resolution precipitation, which contain significant trends and strong intermittency in time domain, are non-stationary [18]. This intrinsic non-stationarity in precipitation series can induce misleading results. Various Hurst estimators are affected by the non-stationary properties [19–21]. So to choose the suitable method analyzing the precipitation records is necessary. Thirdly, the different results are closely linked with different precipitation process and dynamics. For example, the long-term persistence within a storm is very different compared with fluctuations at the seasonal scale. Thus it is useful and appropriate to characterize the LTP behavior within a typical scale range and link the LTP behavior with typical precipitation process [4,22,23].

In this paper, we use finer resolution **instrumental datasets** and suitable method to solve the problems listed above. We use hourly and daily resolution sampled precipitation records over the United States. The high-resolution precipitation records allow us to detect the persistence over smaller time scales, and provide more reliable results, compared with climate simulations and reconstructions. To avoid the spurious results caused by non-stationarity existing in the high-resolution records, DFA is applied here [19–21,24]. It permits the detection of long-range correlations embedded in a seemingly non-stationary time series. In the aspect of dealing with the multiple scaling behaviors, it has also been successfully applied in temperature, wind speeds and so on [8,24]. In this way, we can study the precipitation persistence behavior over a range of temporal scales and identify it is process-dependent. One of the most common methods, power spectrum, is also used in this paper [25,26]. Even though larger fluctuations could increase uncertainties in spectral exponent estimation, it is an effective way to help us verify that the process-dependent long-term persistence in precipitation truly exists. Other estimators, such as R/S, Whittle, which derived under certain assumption, are not suitable here [27–29].

The paper is organized as follows: In Section 2 we describe precipitation data used in this study, the detrended fluctuation analysis method and how robust of DFA on intermittent series. The detailed results from observational data and numerical tests are shown in Section 3. In Section 4, we conclude the results and make a further discussion about the intermittency impacts. We also provide discussion about scale-dependent properties of long-term persistence in other climate variables.

## 2. Data and methods

### 2.1. Data

We use hourly and daily **instrumental** precipitation data across the United States, provided by the National Oceanic and Atmospheric Administration (NOAA). Table 1 summarizes the data resolution, number of series, data length, data source as well as missing value ratio. The missing data are filled up by linear interpolation method [30].

Fig. 1 shows the locations of hourly and daily sampled precipitation gauges used in this paper and one example time series of the hourly and daily records. Even though most of the gauges are not overlapped, they distribute evenly over the United States.

The annual cycle can be found in the hourly and daily precipitation records. The oscillation may lead a false determination of the correlation behavior [24]. In order to remove the periodic annual cycle, we use the anomaly series (whose annual cycle has been removed). Take hourly record as an example, we use  $x'_i = (x_i - \langle x_i \rangle_h) / \sigma_{i,h}$ , where  $x_i$  is the original hourly precipitation series,  $x_{i,h}$  represents the  $h$ th hour precipitation of each year,  $h = 1, 2 \dots 8640$ .  $\langle x_i \rangle_h$

**Table 1**  
Data details we used in the paper.

Resolution	Number of series	Length	Source	Missing value
Hourly	90	39 to 73 years	NOAA <sup>a</sup>	Less than 10%
Daily	13	Nearly 100 years	NOAA <sup>a</sup>	Less than 6%

<sup>a</sup><https://www.ncdc.noaa.gov/cdo-web/datatools/findstation>.

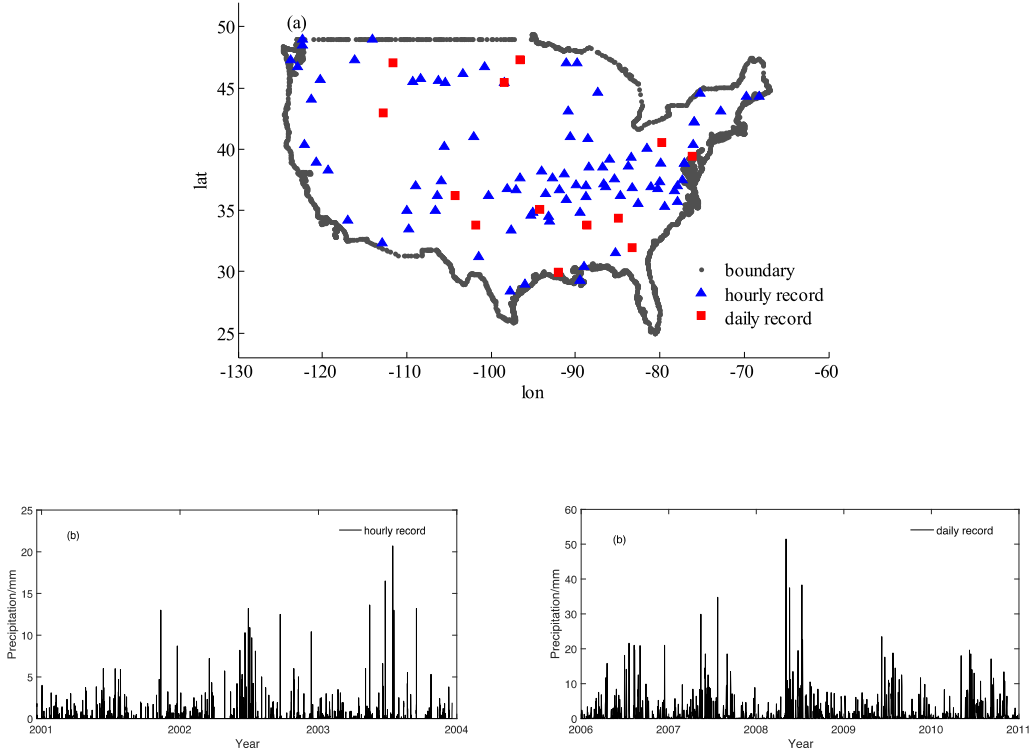


**Fig. 1.** Locations of hourly and daily sampled precipitation gauges we used over the United States (a) and typical time series of the hourly and daily records (b).

represents the mean value of  $h$ th hour precipitation of each year and  $\sigma_{i,h}$  is its standard deviation. If the precipitation is equal to 0 of all  $x_{i,h}$  for a given  $h$ , then the new  $x'_i$  is equal to 0. The annual cycle of daily precipitation is removed by the similar method.

In order to compare the self-consistence of estimated correlation among different resolution sampled precipitation records, the hourly resolution precipitation within a day can be accumulated into daily sampled record and further to bi-weekly sampled record within two weeks.

## 2.2. Method

In order to avoid spurious results caused by non-stationarity in datasets and provide the multiple scaling properties, the DFA is applied here.

There are three steps in DFA algorithm:

(1) Calculate the profile of the time series

$$Y_k = \sum_{i=1}^k x'_i, \quad i = 1, 2, \dots, N$$

(2) The profile series is divided into  $N_s = [N/s]$  non-overlapping segments with equal lengths  $s$ , indexed by  $k = 1, 2, \dots, N_s$ . Since the length of series is not always equally divided exactly, the same procedure should be repeated by the other end of series. In each segment  $s$ , we apply the least square regression method to determine the local trend of each segment and get the  $F_s^2(k)$  as the variance of  $k$ th segment. In this paper, the detrended order is taken as 2.

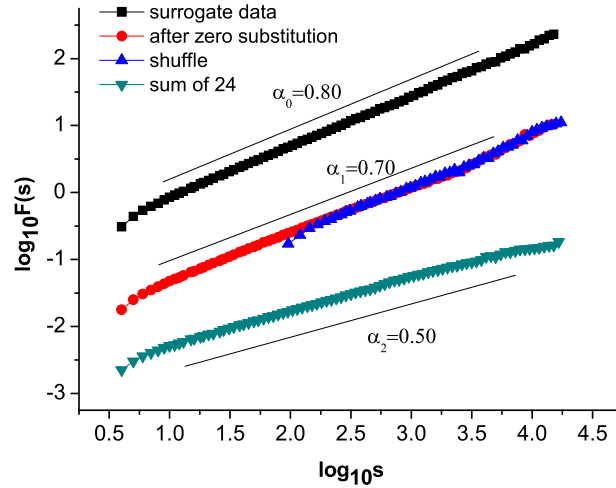


**Fig. 2.** Double log plots of  $F(s)$  vs  $s$  from generated long-term correlated data sets with length  $N = 2^{16}$  (black), truncated data with intermittency pattern of real hourly precipitation anomaly (red), shuffle of the truncated data (green), summed data over 24 non-overlapping windows (blue). Solid black lines are linear fit over corresponding specific ranges.

(3) Average all segments of length, we get the root-mean-square fluctuation.

$$F(s) = \sqrt{\frac{1}{2N_s} \sum_{k=1}^{2N_s} F_s^2(k)}.$$

At the timescale range where the scaling holds,  $F(s)$  increases with time window  $s$  as power law  $F(s) \propto s^\alpha$ . Consequently, the fluctuation  $F(s)$  versus the time scale  $s$  would be depicted as a straight line in the double-logarithmic plot. The slope of the fitted linear regression line is the scaling exponent  $\alpha$ , also called correlation exponent. If  $\alpha = 0.5$ , the time series is uncorrelated. If  $0.5 < \alpha < 1$ , the time series is positively long-term correlated, which also means the long-term persistence exist across the corresponding scale range.

The spectral exponent  $\beta$  based on power spectrum is given by the slope of the least square regression of the power spectrum plotted in log-log scales. Theoretically, the exponents  $\alpha, \beta$  are connected with a relationship:  $\alpha = \frac{1+\beta}{2}$  [21].

In order to confirm our findings are unique features in precipitation, we compare the results with artificially generated long-term correlated data. The artificial data is obtained through Fourier-filtering technique [31]. The spectral exponents of an uncorrelated random data are multiplied by  $f^{-\beta}$ , where the relation between spectral exponent  $\beta$  and DFA exponent  $\alpha$  is  $\beta = 2\alpha - 1$  [21]. The series is then transformed back by inverse Fourier with the modified exponents. The generated series exhibits a power-law correlation over all the time scales.

Intermittency, one of the most obvious features in high-resolution datasets should not be ignored during the LTP studies. To evaluate the robustness of DFA on intermittent series, we simulate a truncated time series. The truncated time series is derived from the generated long-term correlated time series with Generalized Pareto distribution (GPD) (or other distributions, such as normal distribution, will not change the conclusions given in this study), but set some values equal to zero with the same intermittency pattern of the real precipitation anomaly series. The scaling exponent of the generated long-term correlated data is  $\alpha_0 = 0.80$  and the length is  $N = 70128$  which is the same with 8-year hourly precipitation series. Fig. 2 shows the result of truncated series with the real hourly precipitation anomaly intermittency pattern. For comparison, results of the original generated series and the shuffled of the truncated series are also shown. When DFA is applied on both the original and the truncated time series, it turns out that intermittency lead a little bit negative bias of the estimation ( $\alpha_0 = 0.80, \alpha_1 = 0.70$ ). When we shuffle the intermittency pattern, the long-term persistence disappears ( $\alpha_2 = 0.50$ ). Even though the intermittency pattern causes a negative bias for the exponent estimation, the long-term persistence of known time series can also be detected by DFA.

### 3. Results

#### 3.1. Hourly precipitation

Hourly precipitation over a representative meteorological station (Washington in Virginia) is selected to show the results. The time span of the precipitation series is from 1949 to 2013. DFA results show that two dominated scaling ranges (Fig. 3a) are separated by a crossover at around 180 h, where the crossover can be simply determined by the position of maximum residual (MR) in the least-squares fitting  $\log F(s)$  to  $\log s$  (Fig. 3c). The similar crossover position

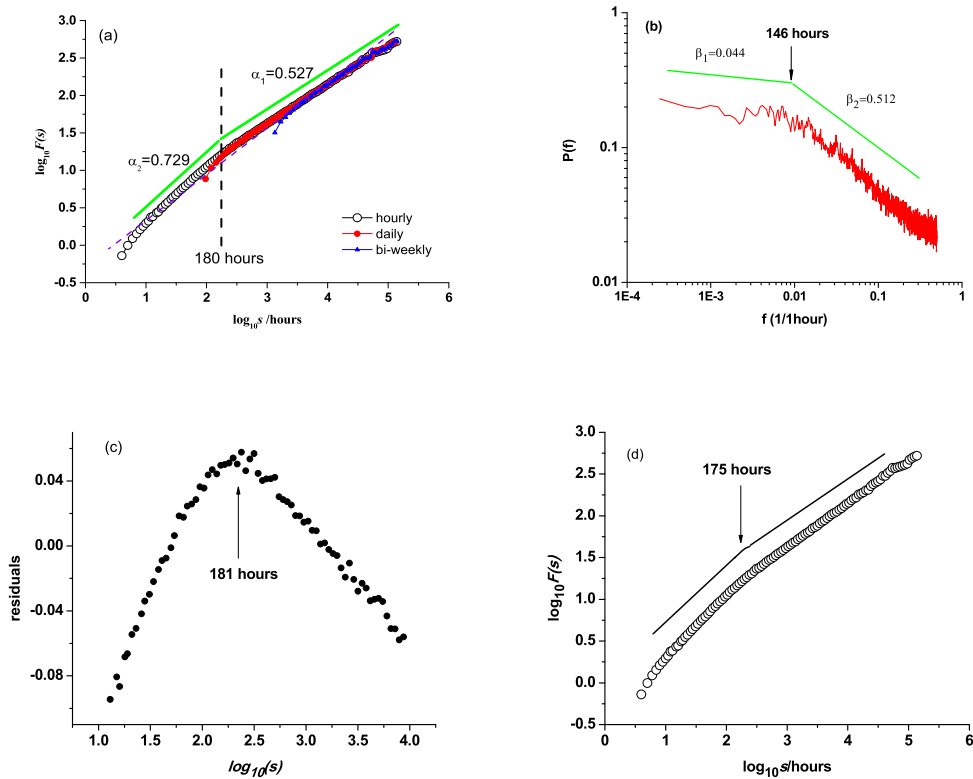


**Fig. 3.** Double log plots of  $F(s)$  vs  $s$  from hourly (hollow), accumulated daily (red) and accumulated bi-weekly (blue) sampled precipitation records (a), and power spectrum from hourly sampled precipitation records (b). Solid green lines are linear fit over corresponding specific ranges and Dash violet lines are linear fit over whole range. Crossover determined by residuals of the linear fit  $\log F(s)$  vs  $\log s$  over the whole scale range from hourly (hollow) (c) and by the multiple-range least regression method (d).

(see Fig. 3d, around 175 h) can also be obtained from multiple-range regression method [32]. Similar dominated scaling ranges and crossover can also be found in the power spectrum analysis (Fig. 3b). However, the large fluctuations in all frequency range will increase larger uncertainties on estimating the scaling exponents and crossover positions. So we can only qualitatively learn the existence of two dominated scaling ranges and crossover by the power spectrum analysis. If we need more quantitative results, the exponents estimated by DFA should be analyzed. Above this crossover (determined by MR method), the exponent is  $\alpha = 0.527$  (i.e.,  $\beta = 0.054$ ), which means a weak correlation at the scale larger than 180 h (Fig. 3a). It is consistent with previous studies that a weakly correlated behavior has been detected at scales larger than 10 days from daily resolution precipitation over Europe [11] and China [13,15]. But when it comes to the shorter time range, something different happened. The exponent increases to  $\alpha = 0.729$  (i.e.,  $\beta = 0.458$ ). It indicates that a strong positive persistence exists at the scale smaller than 180 h. When accumulated daily precipitation data and bi-weekly precipitation data are applied to carry on the same analysis, the lines of  $F(s)$  overlap with the lines obtained from original hourly resolution precipitation (Fig. 3a). With the temporal resolution decreases (more have been accumulated), the long-term correlation structure below the crossover will be reduced. Since the accumulated summation is a kind of filtering, fluctuations on the higher frequency will be smoothed off. The accumulated precipitation will reflect the scaling behavior on the larger time scales, but hide the smaller scales.

The crossover and scaling exponents are variable among stations. For 90 hourly sampled series, most of crossovers are distributed from 150 h to 250 h (nearly 75% among 90 records, see Fig. 4a. The averaged crossover between the two scaling regimes happens around 200 h. Fig. 4b and 4c show the correlation behaviors quantified by scaling exponent  $\alpha$  above and below each specific crossover position from 90 rain gauges in the United States. On the scale above each specific crossover position, most of the exponents fall into the interval between 0.52 and 0.60. In fact, the mean value of scaling exponents for the 90 stations is  $\bar{\alpha} = 0.563$  (i.e.,  $\beta = 0.126$ ) and standard deviation is  $\sigma_\alpha = 0.032$ , indicating a weak long-term persistence. This result is in well accordance with the previous results [11,13] from daily resolution precipitation ( $\bar{\alpha} = 0.54$ ,  $\sigma_\alpha = 0.02$ ) over 739 stations in China. While this is a little bit different from the schematic diagram of scaling regimes of continental European rainfall over range from 1 month to 3 years  $\beta = 0$  (i.e.,  $\alpha = 0.5$  [4]). The difference mainly results from the method of Fourier spectral analysis, which is prone to be biased by the trends or non-stationarity [19–21]. Fig. 4c shows the distribution of scaling exponents below each specific crossover. Most of the exponents fall into the interval between 0.65 and 0.75 with  $\bar{\alpha} = 0.700$ ,  $\sigma_\alpha = 0.051$  (i.e.,  $\beta = 0.400$ ), indicating a

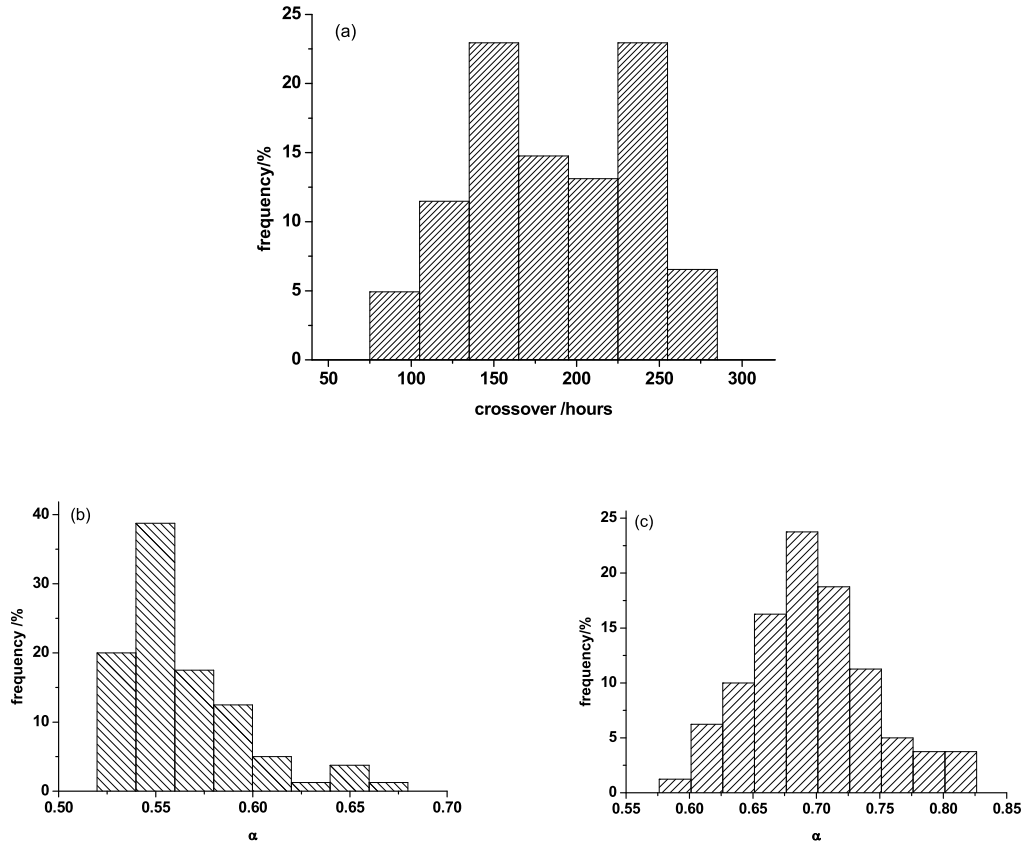


**Fig. 4.** The histograms of the crossover calculated by maximum residuals method from (a) 90 hourly sampled precipitation records. The histograms of the correlation exponents over the scale range (b) larger than each specific crossover and (c) below each specific crossover from 90 hourly sampled precipitation records.

strong long-term persistence. This result is in well accordance with the results suggested from Fourier spectral analysis by Fraedrich and Larnder in their schematic diagram of scaling regimes of continental European rainfall range from 2.4 h to 3 days ( $\beta = 0.5$  i.e.,  $\alpha = 0.75$  [4]).

Thus two distinct scaling regimes are identified, one corresponding to weak long-term persistence and the other to strong long-term persistence, separated by around 200 h. The different scaling behaviors of precipitation may be induced by different physical mechanisms, just like temperature [33,34]. The regime below 200 h is a typical range related to frontal system [4], since the mean duration of warm and cold fronts lasts between 8 and 12 h and the warm front-sector-cold lasts 29 to 34 h. The average recurrence time between successive cold and warm fronts are from 80 to 120 h. So the persistence of precipitation that controlled by frontal system behaves strongly long-term correlated. Above 200 h, there is no larger precipitating system caused by baroclinic instability. It acts like white noise as the passage of weather systems does not appear to show any nontrivial organization. The precipitation process is perhaps mainly dominated by climate variability.

### 3.2. Daily sampled precipitation

In order to investigate the scaling behavior extended to longer time scales, we use 13 long daily precipitation records to analyze the precipitation scaling behaviors range from 9 days to 3 years and above 3 years. Fig. 5 shows the histograms of  $\alpha$  within these two scaling regimes. We cannot find distinct differences between these two regimes. At the scale above 3 years, most of the exponents are about 0.56 (Fig. 5a) ( $\bar{\alpha} = 0.54$ ,  $\sigma_{\alpha} = 0.03$ ). At the scale range from 9 days to 3 years, most of the exponents fall into the interval between  $\alpha = 0.54$  and  $\alpha = 0.55$  (Fig. 5b) ( $\bar{\alpha} = 0.54$ ,  $\sigma_{\alpha} = 0.02$ ). This result is in well accordance with the previous results ( $\bar{\alpha} = 0.568$ ,  $\sigma_{\alpha} = 0.032$ ) given in Fig. 4b from hourly sampled records and the previous results ( $\bar{\alpha} = 0.54$ ,  $\sigma_{\alpha} = 0.03$ ) from daily resolution precipitation over 739 stations in China [13]. However this result is markedly different from the result suggested by Fraedrich and Larnder. They defined a new regime ( $\beta = 0.7$  i.e.,  $\alpha = 0.85$ ) on the range above 3 years, with the method of Fourier spectral analysis [4]. This difference mainly results from the method of Fourier spectral analysis with scattered spectrum in the low frequency range [9], which makes it difficult to reach an objective conclusion.

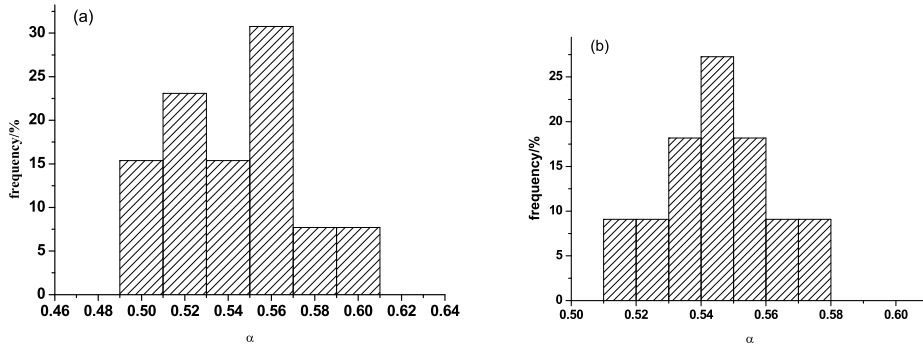


**Fig. 5.** The histograms of the correlation exponents at the scale (a) above 3 years and (b) from 9 days to 3 years from 13 long daily precipitation records.

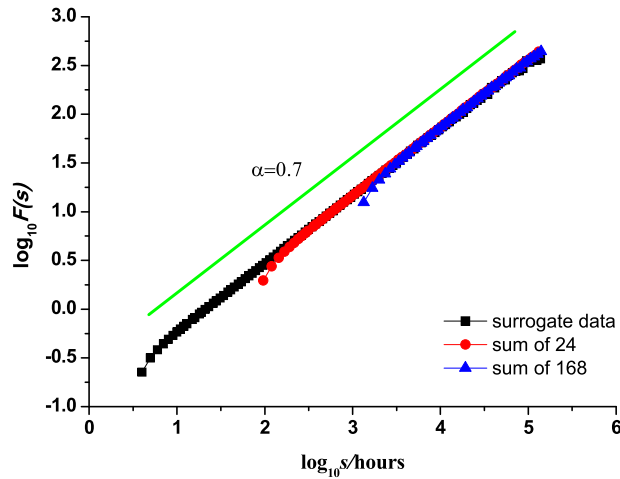


**Fig. 6.** Double log plots of mean  $F(s)$  vs  $s$  from 20 generated long-term correlated data sets of length  $N = 5 \times 10^5$ . (a) surrogate data (black) summed data over 24 non-overlapping windows (red) (c) summed data over 168 non-overlapping windows (blue). Solid green lines are linear fit over corresponding specific ranges.

### 3.3. Accumulation effect and scale dependence

In order to test that the scaling regime behavior is the unique feature found in precipitation and there is no effect on the estimation due to accumulation, we generated linear long-term correlated records using Fourier-filtering technique [31] to model hourly sampled correlated process. Then we summed the generated series over 24 and 168 non-overlapping windows to get the corresponding daily and weekly datasets. Take correlation exponent  $\alpha = 0.70$  as an example, Fig. 6 is the mean detrended variability  $F(s)$  versus scale  $s$  from 20 data sets with length  $N = 5 \times 10^5$ . Detrended variability  $F(s)$  from different resolution samples is coincident with each other on the same range and there is no crossover within the whole range. There is no process-dependent persistence in the idealized correlated process and the accumulation over different windows (different resolutions) will cause no impact on the estimation of correlation exponent.

## 4. Discussions and conclusions

Using the daily precipitation records, many previous studies claim that precipitation possesses a unique scaling behavior, which is uncorrelated or weakly positive correlated. Based on hourly and daily sampled precipitation data, the multiple scaling behaviors over the United States have been analyzed by DFA method. The precipitation **does** possess multiple scaling on sub-ranges rather than a unique scaling behavior. A composite diagram of different scaling regimes averaged by all of the precipitation records with hourly and daily resolutions over the United States is shown in Fig. 7. The similar exponents and crossovers obtained by the two methods make the results more convincing and independent of methodology. The scaling behavior of precipitation process contains two regimes: a regime with stronger LTP (around  $12 \text{ h} < s < 200 \text{ h}$ ,  $\alpha \approx 0.74$ ) and a regime with weaker LTP (around  $200 \text{ h} < s < 24 \text{ years}$ ,  $\alpha \approx 0.54$ ).

Two distinct scaling regimes with different correlation structures correspond to different processes in precipitation. The process with the time scale less than 200 h represents frontal system [4] [9]. Within this scale range, the mean value

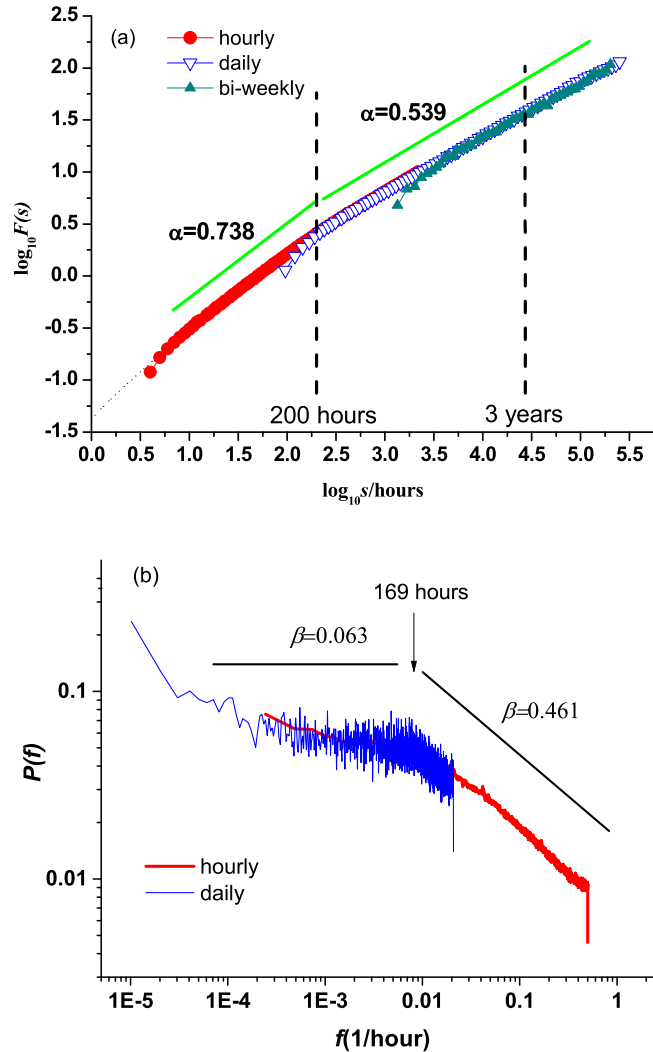


**Fig. 7.** Composite diagram calculated from ensemble averaged DFA (a) and power spectra (b) of all available precipitation series used in this study the scaling regimes of precipitation over the United States from multiple resolutions (90 hourly and 13 daily) sampled precipitation variability. Solid green lines are linear fit over corresponding specific ranges.

for scaling exponent is close to 0.7, indicating strong long-term persistence. In this case, a strongly positive long-term correlated process should be used to model the frontal systems [35].

The process with the time scale starts from around 200 h is regarded as random nature of weather systems and climate variability. Within this scale range, the mean value for correlation exponents is about 0.55, indicating a weakly long-term persistence process. In that case, Markov process can be used to model the precipitation at large time scales [3,4,12,36].

We conclude that the long-term persistence of precipitation is process-dependent. When we simulate the precipitation process over the different scales, it is necessary to emphasize the different persistence properties over the corresponding scale.

It has not well known enough that how the presence of zero values may considerably affect the LTP of precipitation, even though it has been noticed for a long time [37,38]. Recently, De Montera advocated the presence of zeros lead to a break in the scaling at 1 h time scale when they performed the scaling analysis of high resolution time series [39]. Verrier et al. compared the scaling behavior of uninterrupted rain series (with almost zeros) and rain events and found zero values of rainfall will strongly affect the scaling properties at large scales [40]. There is also intrinsic information existing in the rain-no rain pattern.

Precipitation is not the only variable which presents such process dependent feature. It has been suggested [41] that the atmospheric fluctuation contains 5 scaling regimes: a regime of weather ( $s < 10$  days,  $\alpha \sim 0.75$ ), a regime of macro-weather ( $10$  days  $< s < 50$  years,  $\alpha \sim -0.2$ ), a regime of climate ( $50$  years  $< s < 80$  kyrs,  $\alpha \sim 0.4$ ), a regime of macroclimate ( $80$  kyrs  $< s < 0.5$  Myrs,  $\alpha \sim -0.8$ ), a regime of mega-climate ( $s > 0.5$  Myr,  $\alpha \sim 0.4$ ). As we move from one regime to

the next, the scaling exponent alternates in sign and magnitudes. The transition scale of around 10 days can be predicted by the scaling of the turbulent wind due to solar forcing [42]. Similar phenomenon also occurs in paleo-temperature records between glacier and inter-glacier time scales [36]. The Holocene and the glacial climates have distinctly different scaling properties. The Holocene is mono-fractal with a scaling exponent  $\alpha \sim 0.7$ . On the contrary, the glacial climate is multi-fractal with  $\alpha \sim 1.2$ , indicating a longer persistence time and the stronger nonlinearities. When entering the glacial climate state and even longer time scales, a scale break is observed at the Milankovitch time scale (around 20 kyr). When the scale is longer than 20 kyr, a trivial scaling with a Hurst exponent close to 0.5 is found. The scale-dependent properties of long-term correlation occur at the wind speed as well. For temporal scales longer than one day, the scaling exponent is greater than 0.5. For shorter time scales, the scaling exponent is close to unity, which is characteristic of  $1/f$  noise [32,43,44]. Precipitation and wind time series are similar in some aspects. For example, dry and wet spells in precipitation records correspond to windy and calm spells in wind spells records. So the possible reason for wind speed crossover occurrence is also due to the multiple temporal scaling characteristics.

## Acknowledgments

The authors acknowledge the supports from the National Natural Science Foundation of China (41675049 and 41475048). We thank Dr. Christian L.E. Franzke for discussions and Sebastian Schubert, Yumeng Chen for grammar suggestions.

## References

- [1] E. Koscielny-Bunde, A. Bunde, S. Havlin, H.E. Roman, Y. Goldreich, H.J. Schellnhuber, Indication of a universal persistence law governing atmospheric variability, *Phys. Rev. Lett.* 81 (3) (1998) 729.
- [2] H.E. Hurst, The problem of long-term storage in reservoirs, *Int. Assoc. Sci. Hydrol. Bull.* 1 (3) (1956) 13–27.
- [3] K.W. Potter, Annual precipitation in the Northeast United States: Long memory, short memory, or no memory? *Water Resour. Res.* 15 (2) (1979) 340–346.
- [4] K. Fraedrich, C. Larnder, Scaling regimes of composite rainfall time-series, *Tellus A* 45A (1993) 289–298.
- [5] J. Beran, *Statistics for Long-Memory Processes*, Chapman & Hall/CRC, New York, 1994.
- [6] N.M. Yuan, Z.T. Fu, J.Y. Mao, Different scaling behaviors in daily temperature records over China, *Physica A* 389 (19) (2010) 4087–4095.
- [7] M. Bogachev, A. Bunde, Universality in the precipitation and river runoff, *Europhys. Lett.* 97 (4) (2012) 48011.
- [8] N.M. Yuan, Z.T. Fu, Century-scale intensity modulation of large-scale variability in long historical temperature records, *J. Clim.* 27 (4) (2014) 1742–1750.
- [9] C. Matsoukas, S. Islam, I. Rodriguez-Iturbe, Detrended fluctuation analysis of rainfall and stream flow time series, *J. Geophys. Res.* 105 (D23) (2000) 29165–29172.
- [10] A. Bunde, S. Havlin, Power-law persistence in the atmosphere and in the oceans, *Physica A* 314 (1) (2002) 15–24.
- [11] J.W. Kantelhardt, E. Koscielny-Bunde, D. Rybski, P. Braun, A. Bunde, S. Havlin, Long-term persistence and multifractality of precipitation and river runoff records, *J. Geophys. Res.* 111 (D1) (2006) 01106.
- [12] A. Bunde, U. Buntgen, J. Ludescher, J. Luterbacher, H. von Storch, Is there memory in precipitation? *Nature Clim. Change* 3 (3) (2013) 174–175.
- [13] L. Jiang, N. Li, X. Zhao, Scaling behaviors of precipitation over China, *Theor. Appl. Climatol.* 128 (2017) 63–70.
- [14] S. Faticchi, Y. V. Ivanov, E. Caporali, Investigating interannual variability of precipitation at the global scale: Is there a connection with seasonality? *J. Clim.* 25 (2012) 5512–5523.
- [15] S.S. Zhao, W.P. He, Evaluation of the performance of the Beijing Climate Centre Climate System Model 1.1(m) to simulate precipitation across China based on long-range correlation characteristics, *J. Geophys. Res.: Atmos.* 120 (24) (2015) 12576–12588.
- [16] Y. Markonis, D. Koutsoyiannis, Scale-dependence of persistence in precipitation records, *Nature Clim. Change* 6 (4) (2016) 399–401.
- [17] V. Livina, S. Havlin, A. Bunde, Memory in the occurrence of earthquakes, *Phys. Rev. Lett.* 95 (20) (2005) 208501.
- [18] L.M. Canel, J.I. Katz, Trends in US hourly precipitation variance 1949–2009, *J. Hydrometeorol.* 19 (3) (2018) 599–608.
- [19] C.K. Peng, S. Buldyrev, M. Simons, H. Stanley, A. Goldberger, Mosaic organization of DNA nucleotides, *Phys. Rev. E* 49 (2) (1994) 1685–1689.
- [20] C.K. Peng, J.M. Hausdorff, S. Havlin, J.E. Mietus, H.E. Stanley, A.L. Goldberger, Multiple-time scales analysis of physiological time series under neural control, *Physica A* 249 (1) (1998) 491–500.
- [21] P. Talkner, R.O. Weber, Power spectrum and detrended fluctuation analysis: Application to daily temperatures, *Phys. Rev. E* 62 (1) (2000) 150–160.
- [22] M. Marani, On the correlation structure of continuous and discrete point rainfall, *Water Resour. Res.* 39 (5) (2003) 1128.
- [23] G. Poveda, Mixed memory, (non) Hurst effect, and maximum entropy of rainfall in the tropical andes, *Adv. Water Resour.* 34 (2) (2011) 243–256.
- [24] J.W. Kantelhardt, E. Koscielny-Bunde, H.H.A. Rego, S. Havlin, A. Bunde, Detecting long-range correlations with detrended fluctuation analysis, *Physica A* 295 (3) (2001) 441–454.
- [25] Y. Tessier, S. Lovejoy, P. Hubert, D. Schertzer, S. Pecknold, Multifractal analysis and modeling of rainfall and river flows and scaling, causal transfer functions, *J. Geophys. Res.* 1012 (21) (1996) 26427–26440.
- [26] F. Fabry, On the determination of scale ranges for precipitation fields, *J. Geophys. Res.* 101 (D8) (1996) 12819–12826.
- [27] M. Taqqu, V. Teverovsky, W. Willinger, Estimators for long-range dependence: An empirical study, *Fractals* 3 (4) (1995) 785–798.
- [28] L. Bisaglia, D. Gan, A comparison of techniques of estimation in long-memory processes, *Comput. Statist. Data Anal.* 27 (1) (1998) 61–81.
- [29] M.S. Taqqu, V. Teverovsky, Robustness of whittle-type estimators for time series with long-range dependence, *Commun. Stat. Stoch. Model.* 13 (4) (1997) 723–757.
- [30] P.S. Wilson, A.C. Tomsett, R. Toumi, Long-memory analysis of time series with missing values, *Phys. Rev. E* 68 (1) (2003) 017103.
- [31] H. Makse, S. Havlin, M. Schwartz, H. Stanley, Method for generating long-range correlations for large systems, *Phys. Rev. E* 53 (5) (1996) 5445–5449.
- [32] M.D.O. Santos, T. Stosic, B.D. Stosic, Long-term correlations in hourly wind speed records in pernambuco, Brazil, *Physica A* 391 (4) (2012) 1546–1552.
- [33] K.M. van Vliet, A. van der Ziel, R.R. Schmidt, Temperature-fluctuation noise of thin films supported by a substrate, *J. Appl. Phys.* 51 (6) (1980) 2947–2956.

- [34] J.D. Pelletier, The power spectral density of atmospheric temperature from time scales of 10–2 to 106 yr, *Earth Planet. Sci. Lett.* 158 (3–4) (1998) 157–164.
- [35] B.B. Mandelbrot, J.W. Van Ness, Fractional Brownian motions, fractional noises and applications, *SIAM Rev.* 10 (1968) 422–437.
- [36] Z.G. Shao, P. Ditlevsen, Contrasting scaling properties of interglacial and glacial climates, *Nature Commun.* 7 (10951) (2016).
- [37] D. Harris, M. Menabde, A. Seed, G. Austin, Multifractal characterization of rain fields with a strong orographic influence, *J. Geophys. Res.: Atmos.* 101 (D21) (1996) 26405–26414.
- [38] F. Schmitt, S. Vannitsem, A. Barbosa, Modeling of rainfall time series using two-state renewal processes and multifractals, *J. Geophys. Res.: Atmos.* 103 (D18) (1998) 23181–23193.
- [39] L. De Montera, L. Barthès, C. Mallet, P. Golé, The effect of rain–no rain intermittency on the estimation of the universal multifractals model parameters, *J. Hydrometeorol.* 10 (2) (2009) 493–506.
- [40] S. Verrier, C. Mallet, L. Barthès, Multiscaling properties of rain in the time domain, taking into account rain support biases, *J. Geophys. Res.: Atmos.* 116 (D20) (2011) D20119.
- [41] S. Lovejoy, A voyage through scales, a missing quadrillion and why the climate is not what you expect, *Clim. Dynam.* 44 (2015) 3187–3210.
- [42] S. Lovejoy, D. Schertzer, Towards a new synthesis for atmospheric dynamics: space–time cascades, *Atmos. Res.* 96 (1) (2010) 1–52.
- [43] R.G. Kavasseri, R. Nagarajan, Evidence of crossover phenomena in wind-speed data, *IEEE Trans. Circuits Syst. I. Regul. Pap.* 51 (11) (2004) 2255–2262.
- [44] R.B. Govindan, H. Kantz, Long-term correlations and multifractality in surface wind speed, *Europhys. Lett.* 68 (2) (2004) 184–190.